Measurements of Moisture Diffusivity for Porous Building Materials

R.F. Richards, Ph.D.

ABSTRACT

Moisture diffusivities of several common porous building materials were determined experimentally. Both wood-based and inorganic materials were included in the study. A steady-flux method was used that involved determining the one-dimensional moisture content profile produced in a sample through which a known constant flux of water is flowing. The transient mass fluxes through samples upon exposure to water, steady-state mass fluxes, one-dimensional moisture content profiles, and capillary pressure curves for low suction pressures, as well as the moisture diffusivities for a range of moisture contents, are presented for each material. Results of the study are compared to previously published measurements for similar materials.

INTRODUCTION

The accumulation of moisture in porous building materials may lead to both material degradation and reduction of the insulating value of the building envelope. In order to identify good design and construction practices, it is important to come to a clearer understanding of how moisture invades building components.

Recently the development of mathematical models aimed at predicting moisture migration in wall systems has been reported by Kohonen (1984a), Spolek et al. (1985), Pedersen (1990), and Burch and Thomas (1991). For all of these models, the lack of reliable property data has become an impediment to widespread application.

For this reason, NIST has embarked on a systematic program to measure the moisture transport properties necessary to fully characterize the hygro-thermal behavior of common building materials. Other papers have dealt with measurements of vapor permeability and sorption isotherms made at NIST (see Burch et al. [1992] and Richards et al. [1992]). The present study extends the data base to include liquid transport properties for porous building materials. Measurements of capillary pressure under wetting conditions, time histories of mass flux through sample materials upon exposure to liquid water, one-dimensional moisture content profiles under steady-flux conditions, and moisture diffusivity functions for a range of moisture contents are presented for gypsum wall board, sugar pine, microfine particle board, and exterior plywood siding.

BACKGROUND

Moisture transport within porous building materials occurs by a combination of several physical mechanisms. Vapor diffusion through gas-filled pores, bound water diffusion along the solid walls of the pores, and the surface tension driven flow of liquid water in partially filled capillary pores may all contribute to the overall mass flux. Since in most practical situations it is not possible to distinguish between the different transport processes, it is common engineering practice to lump the three mechanisms together and describe only the sum of their effects. Often the local moisture content is assumed to be the driving potential and predictions are made using the time-dependent nonlinear diffusion equation:

$$\frac{\partial \gamma}{\partial t} = -\nabla \{\rho D(\gamma) \nabla \gamma\} . \qquad (1)$$

Implicit in Equation 1 is the assumption of isothermal conditions. The variable γ is the local moisture content in kg/kg and ρ is the density of water. $D(\gamma)$ is defined to be a moisture diffusivity with dimensions of m^2/s and an explicit dependence on moisture content. The dependence of the moisture diffusivity on moisture content considerably complicates both the solution of Equation 1 and the experimental task of specifying $D(\gamma)$.

In the past, measurements of moisture diffusivity for soils (Bruce and Klute 1956), sand (Wang and Fang 1988), cementitious building materials (Gummerson et al. 1979), and insulation materials (Frietas et al. 1991) have often indicated an exponential dependence on moisture content in the regime where liquid transport dominates. The method used in each of these studies to determine the functional form of $D(\gamma)$ has been the transient method. To determine $D(\gamma)$ using the transient method, liquid water is brought into contact with one end of a dry specimen of the sample material. The one-dimensional transient moisture content profile is observed over time as water migrates into the sample in an unsteady fashion.

Observation of the transient moisture content profile typically involves the use of a noninvasive and nondestructive moisture content measurement technique so that the moisture profile in a given sample can be determined more than once. To meet this requirement, much inventiveness has gone into the development of more sophisticated nondestructive methods to measure moisture content profiles.

R.F. Richards is an NIST/ASEE postdoctoral fellow in the Heat Transfer Group, Building and Fire Research Laboratory, National Institute of Standards and Technology, Gaithersburg, MD.

Gamma ray absorption has been described by Kohonen (1984b), Kumaran and Bomberg (1985), Quenard and Sallee (1989), and Frietas et al. (1991). Prazak et al. (1990) reported the use of neutron radiography, Ambrose et al. (1990) the use of X-ray radiography, and Gummerson et al. (1979) the use of nuclear magnetic resonance (NMR) imaging.

However, regardless of the technique employed, the essential details of the transient method are unchanged. Once the transient moisture content profile or profiles for a given sample have been obtained, they are plotted together using the Boltzmann similarity variable $\eta = x/\sqrt{t}$. Employing this variable in conjunction with the time-dependent diffusion equation (Equation 1) yields the transformed equation:

$$D(\gamma) = -\frac{1}{2\frac{d\gamma}{d\eta}}\left[\eta\,\gamma(\eta) - \int_{\gamma_{max}}^{\gamma} \eta(\gamma)d\gamma\right], \qquad (2)$$

where moisture diffusivity $D(\gamma)$ is seen to depend both on the reciprocal of the first derivative of γ with respect to η and the integral of the inverse moisture content profile. If the process under study is a diffusion process (i.e., it satisfies Equation 1), then the transient moisture content profiles should collapse together when plotted versus the similarity variable, η. This has been shown to be true for many porous materials (Hall et al. [1983]; Wang and Fang [1988]).

Although the description of moisture transport as driven by gradients in moisture content is often assumed, the true driving potential is known to be capillary pressure when liquid transport dominates at high moisture contents. For this reason, the relation between capillary pressure and moisture content is necessary if moisture diffusivity is to be developed from theoretical considerations. Measurements of capillary pressure over a range of moisture contents have been reported for southern pine by Spolek and Plumb (1981) and for a variety of soft and hardwoods by Choong and Tesoro (1989). Both sets of researchers started out with saturated wood samples and used centrifuging of the samples to measure capillary pressure curves under conditions of decreasing moisture content.

An additional quantity has proved useful in characterizing moisture transport in building materials: the sorptivity. When liquid water is initially introduced to a porous material, the cumulative mass of water pulled into the material per unit area by capillary forces has been found to increase proportionally to the square root of elapsed time (Hall et al. [1983]). The constant of proportionality is the sorptivity, S, and is defined by the relation

$$M = \rho a S\sqrt{t}\,, \qquad (3)$$

where M is the total mass of water absorbed into the material, a is the cross-sectional area, ρ is the density of water, and t is elapsed time.

Assuming an exponential form for moisture diffusivity (in accordance with the earlier experimental evidence),

$$D(\gamma) = D_{sat}\exp\left[c\left(\frac{\gamma}{\gamma_{sat}} - 1\right)\right], \qquad (4)$$

Brutsaert (1976) was able to show that sorptivity could be calculated by

$$S = \sqrt{2\frac{\rho_s}{\rho}\gamma_{sat}D_{sat}\left[\frac{2c-1}{2c^2}\right]\left[\frac{1-e^{-c}}{2c-1}\right]\sum_{n=0}^{\infty}\frac{c^n}{(2n-1)(n!)}}\,. \qquad (5)$$

Equation 5, now known as the Brutsaert approximation, provides a useful connection between sorptivity and moisture diffusivity as long as the assumption of an exponential diffusivity (Equation 4) is not violated.

In the present study, a steady-flux method was developed to avoid the requirement for sophisticated and expensive nondestructive moisture content measurement techniques. Rather than measuring moisture content profiles as they developed in samples undergoing a transient invasion of water, profiles were found only after the flux through a sample had reached a steady state. A steady-state condition was achieved by allowing the liquid water introduced at one end of a sample to leave the sample at the far end by evaporating into the ambient air. Once the mass flux through a sample was known to be constant, the one-dimensional moisture content profile was assumed to be unchanging. Using a simple "cut and weigh" technique similar to that described by Bruce and Klute 1956, the steady-flux moisture content profile in the sample was determined. With the mass flux through the sample constant, the storage term in Equation 1 goes to zero. Solving for diffusivity gives

$$D(\gamma) = -\frac{1}{\rho\frac{d\gamma}{d(mx)}}\,. \qquad (6)$$

For the steady-flux case, moisture diffusivity is seen to be determined by the reciprocal of the first derivative $d\gamma/d(mx)$ where m is the mass flux through the specimen. The product of mass flux and position appears as a natural grouping in Equation 6.

EXPERIMENT

Moisture Content Measurements

Sample specimens were prepared from commercially available lots of material. Sheets of gypsum wallboard, microfine particle board, and exterior plywood sheathing (hereafter referred to as T111 sheathing) and planks of sugar pine were purchased at a local lumberyard. The gypsum wallboard (with paper facings removed) had a density of 670 kg/m^3, the sugar pine a density of 370 kg/m^3, the microfine particle board (with outer surfaces

sanded off) a density of 760 kg/m^3, and the plywood sheathing a density of 590 kg/m^3.

Sample materials were cut into specimens with square cross sections of approximately 10 × 10 mm and lengths between 40 and 100 mm. During the experiment, moisture flowed through each specimen parallel to the specimen's long dimension. The sugar pine was cut with the grain parallel to the specimens' long dimension so that moisture flowed with the grain. The specimens of gypsum, particle board, and plywood sheathing were prepared with their long dimension in the plane of the sheet from which they were cut. For these specimens, moisture flowed parallel to the plane of the sheet.

Distilled water was supplied to each specimen from a burette via plastic tubing epoxied to the base of the specimen. Moisture traveled from the base to the tip of each specimen. The tip was left exposed to laboratory air so that moisture could evaporate freely (See Figure 1). The four long sides of each of the samples were wrapped in 0.025-mm-thick polyethylene film to prevent moisture loss. Care was taken to wrap the specimens very tightly to avoid leaving a path for parallel flow between the specimens and the polyethylene film. The slight swelling of the specimens upon wetting aided in this task.

The burette was used to measure the volume of liquid imbibed into the specimen. In addition, adjusting the relative height of a specimen above the burette allowed control of the suction pressure and, consequently, the moisture content at the base of the specimen. When a specimen could not sustain the suction pressure applied at its base without leaking air into the water supply, absorbent paper was used to wick water from the burette to the specimen. The highest suction pressure applied with plastic tubing only was 10 cm of water and with the paper wick was 25 cm of water. The appearance of gases that had been dissolved in the water, coming out of solution, did not pose a problem. Small bubbles were sometimes observed to form in the supply tubes but did not grow significantly during the experiments.

An experiment began by filling the burette and thereby exposing the base of a dry specimen to water. The flow of water into the specimen was monitored by periodically reading the liquid level in the burette. The liquid levels were read several times a day over the course of an experiment, which lasted from three to thirty days. The temperature and relative humidity in the lab were checked every day and remained constant at 24 ± 1°C and 30 ± 10%, respectively, throughout the experiments.

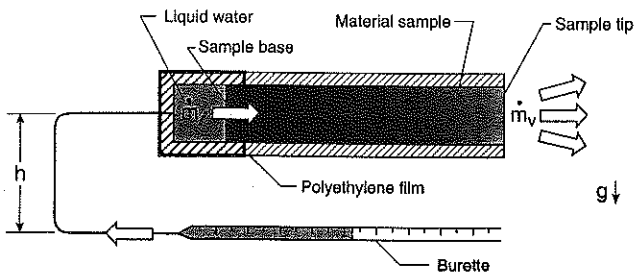

Figure 1 Experimental apparatus.

As water invaded an initially dry specimen, a wet front was seen to move down the specimen. When the wet front advanced to the tip of the specimen, moisture began to leave the specimen by evaporation into the ambient air. The mass flux through a specimen reached a constant value after the rate at which moisture leaving the tip of the specimen by evaporation equaled the rate at which water was being pulled into the base of the specimen. Parallel flow of liquid between the specimens and their polyethylene film covers was not observed but cannot be ruled out. Due to the tight fit achieved in wrapping the specimens, any parallel flow would necessarily be quite small.

Once the mass flux into the specimen was known to be constant, the specimen was disconnected from its water supply and quick-frozen in liquid nitrogen. The frozen specimen was then cut into slices, each 3 to 5 mm thick, using a small rotary saw. The saw blade used was 0.4 mm thick and consistently produced a 0.7-mm-thick saw kerf. Each slice was placed in its own numbered weighing dish, covered, and immediately weighed to determine its wet mass. The dry mass for each slice was subsequently found by weighing the slice after being dried over CaCl desiccant. All weighing was done on a precision balance with a least count of 0.0001 grams. The moisture content of each slice was then determined from

$$\gamma = \frac{(M_w - M_d)}{M_d}, \qquad (7)$$

where M_w and M_d are the slice's wet and dry mass, respectively. The thickness of each slice was measured with a micrometer after the dry mass had been determined. An analysis of the uncertainties in the measurements of local moisture content, slice thickness, and specimen mass flux is discussed in the appendix.

Capillary Pressure Measurements

Capillary pressure curves for wetting were found for each of the four materials. The experimental setup used to make the measurements is shown in Figure 2. Samples of each material, approximately 1 cm^3, were embedded in an absorbent paper wick, approximately 70 cm long. The samples were equally spaced about 5 cm apart over the 70-cm length. The paper wick with embedded samples was then wrapped in a sheet of polyethylene film and secured to a wooden meter stick with tacks. The meter stick was stood vertically in a beaker filled with distilled water.

Over the course of several weeks, free liquid from the beaker was pulled up the absorbent paper wick by capillary action, soaking into the material samples in a wetting process. The surrounding plastic film served to eliminate evaporation from the wick. Upon reaching the top of the

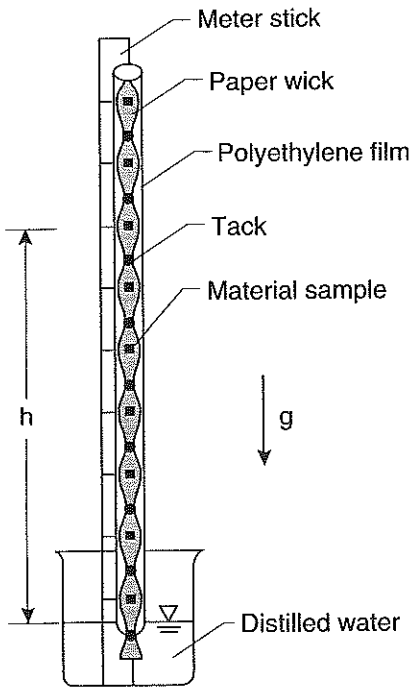

Figure 2 *Measurement of capillary pressure.*

wick, the water in the wick attained a state of hydrostatic equilibrium such that the suction pressure in any given sample was equal to the head of water from the free liquid surface to that sample. Moisture contents were subsequently measured by removing the samples from the wick and weighing them first wet and then again dry. Drying was done using CaCl desiccant. The capillary pressure curve was plotted as suction head in atmospheres as a function of measured moisture content.

RESULTS AND DISCUSSION

Specimen Time Histories

The time histories of gypsum and sugar pine specimens are plotted in Figure 3. Figure 4 shows the time histories of particle board and T111 sheathing specimens. The graphs clearly show two regimes for each specimen. First there is the initial transient behavior as water invades the dry specimen. During this time, the mass of water absorbed into the sample increases as the square root of time. The solid curves on the figures are least-squares linear fits to the equation

$$M = \rho a S \sqrt{t} + b \tag{8}$$

where S is the specimen sorptivity and b is an arbitrary constant introduced to take care of offsets in the starting time.

A second regime begins as the wet front approaches the tip of the specimen and moisture begins to leave the sample by evaporation. The mass flux through the specimen reaches a constant value when the rate at which water being

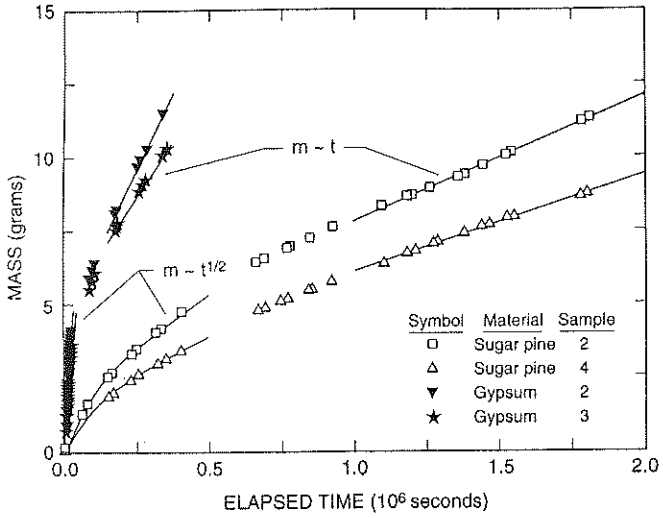

Figure 3 *Time history of sugar pine and gypsum samples showing transient and steady-flux regimes.*

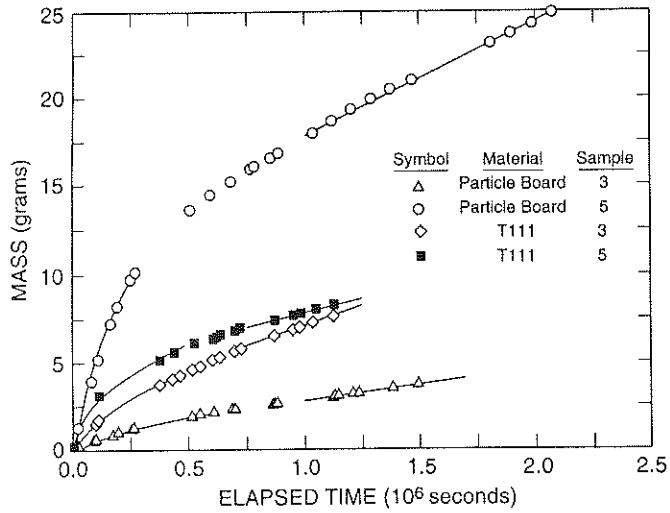

Figure 4 *Time history of particle board and T111 sheathing samples showing transient and steady-flux regimes.*

pulled into the base of the specimen is balanced by the rate at which moisture leaves the tip of the specimen by evaporation. The constant mass flux seen at later times in Figures 3 and 4 indicates that moisture is no longer being stored in the specimens and that change in the moisture content profiles in the specimens has ceased.

Moisture Content Profiles

One-dimensional moisture content profiles for gypsum, sugar pine, particle board, and T111 sheathing after the attainment of a condition of constant mass flux are given in Figures 5, 6, 7, and 8, respectively. Each figure shows a plot of individual-slice moisture contents versus the product of slice distance from the sample tip and mass flux. The

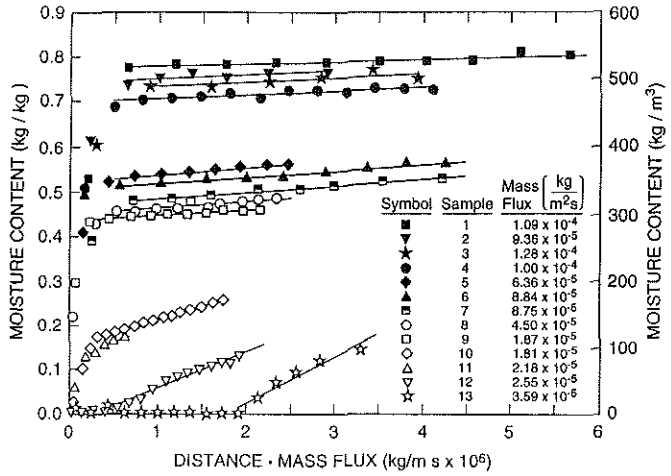

Figure 5 *Measured moisture content profiles for gypsum samples.*

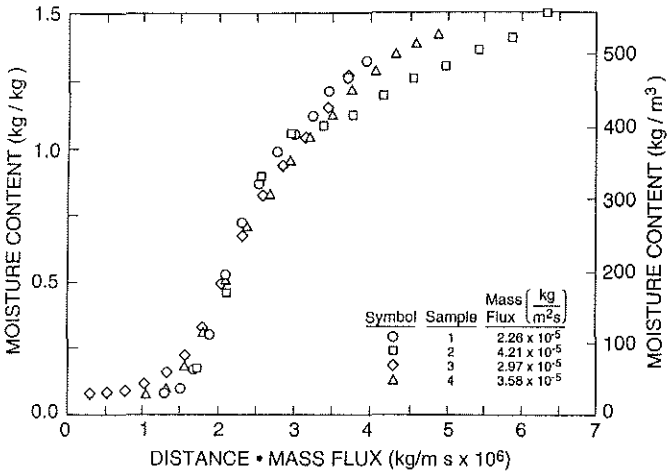

Figure 6 *Measured moisture content profiles for sugar pine samples.*

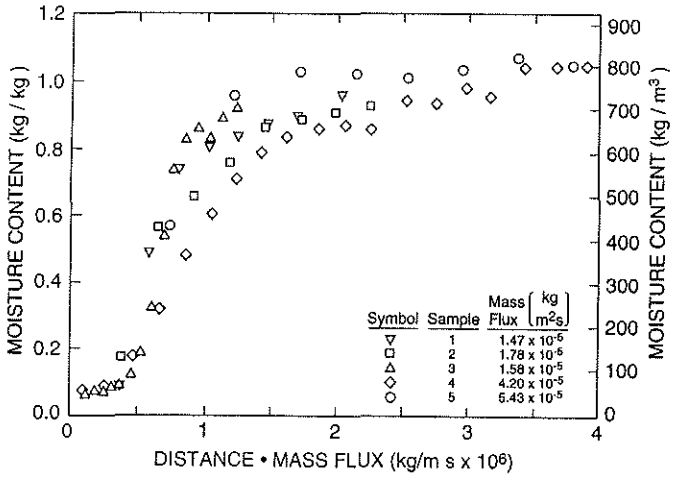

Figure 7 *Measured moisture content profiles for particle board samples.*

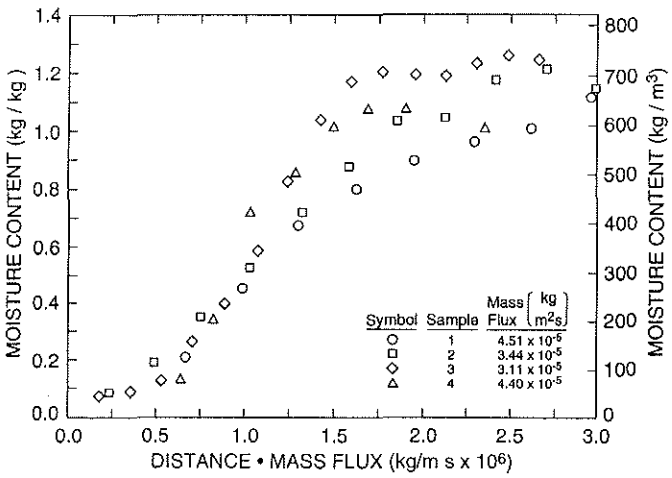

Figure 8 *Measured moisture content profiles for T111 samples.*

choice of abscissa is motivated by the form of Equation 6. The mass flux associated with each profile and used to calculate the abscissas is identified on the figures. It is interesting to note that taking the transpose of each of these figures (i.e., reversing ordinate and abscissa) gives a plot of the flow potential as identified by Arfvidsson and Claesson (1989) and used in their mass transfer computations.

The moisture content profiles for the wood-based materials—sugar pine, particle board, and T111 sheathing, shown in Figures 6, 7, and 8—are all similar in appearance. These profiles take the form of fairly smooth curves with small slopes at low moisture contents ($\gamma < 0.2$ kg/kg), steeper slopes at intermediate moisture contents, and diminishing slopes at higher moisture contents ($\gamma > 0.8$ to 1.0 kg/kg). Scatter in the moisture content profiles is large. The sugar pine data fall in a fairly narrow band, while the particle board and T111 sheathing data show considerably more spread. For all three materials, the greatest scatter in the data seems to occur at the higher moisture contents.

The moisture content profiles for gypsum, shown in Figure 5, are quite different. The profiles that lie above $\gamma = 0.2$ kg/kg are linear with small slopes from the bases of the samples to very close to the tips of the samples. Near the tips of the samples, moisture contents drop off sharply. The slopes of the linear parts of the moisture content profiles are smallest for those profiles at the highest moisture contents and become progressively larger for samples at lower moisture contents. The gypsum sample profiles that lie below a moisture content of $\gamma = 0.2$ kg/kg are more reminiscent of the hygroscopic materials. These profiles are seen to be smoother curves with less drop-off near the sample tips. Scatter in the gypsum moisture content profiles appears smaller than for the other three materials.

Moisture Diffusivity

Moisture diffusivities for gypsum, sugar pine, particle board, and T111 sheathing are given in Figures 9, 10, 11, and 12, respectively. The semi-log plots show moisture diffusivity versus moisture content where the values of moisture diffusivity have been calculated by applying Equation 3 to the moisture content profiles given in Figures 5, 6, 7, and 8. The derivatives needed to evaluate Equation 3 were determined from the moisture content profiles using one of two methods.

In Figure 9 the derivative needed to compute each diffusivity datum for gypsum was found from the slope of a least-squares fit of the linear part of one of the moisture content profiles. These linear fits are indicated in Figure 5 with solid lines. In this case, each profile in Figure 5 yielded one data point on Figure 9.

For Figures 10, 11, and 12, each diffusivity datum was found by fitting a least-squares line to four consecutive points in the moisture profile of a given sample. Successive values of diffusivity were found by shifting the least-squares fit over one point at a time. This procedure resulted in the

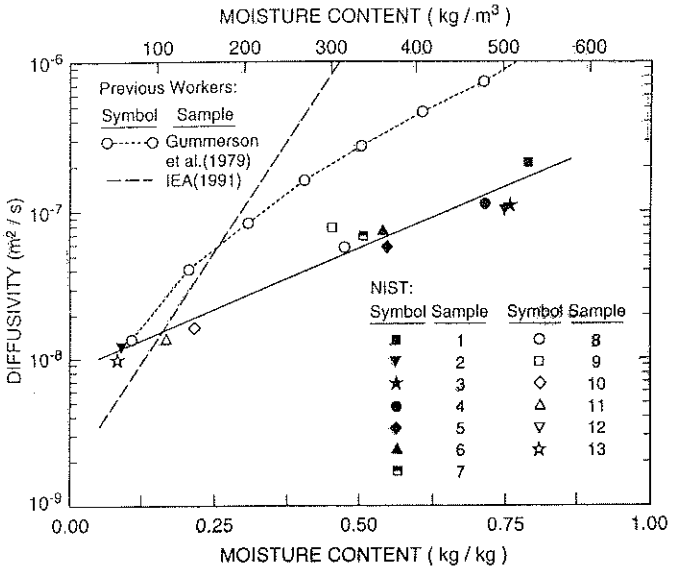

Figure 9 *Moisture diffusivity vs. moisture content for gypsum wall board with gypsum plaster data from VMIST and gypsum correlation from IEA.*

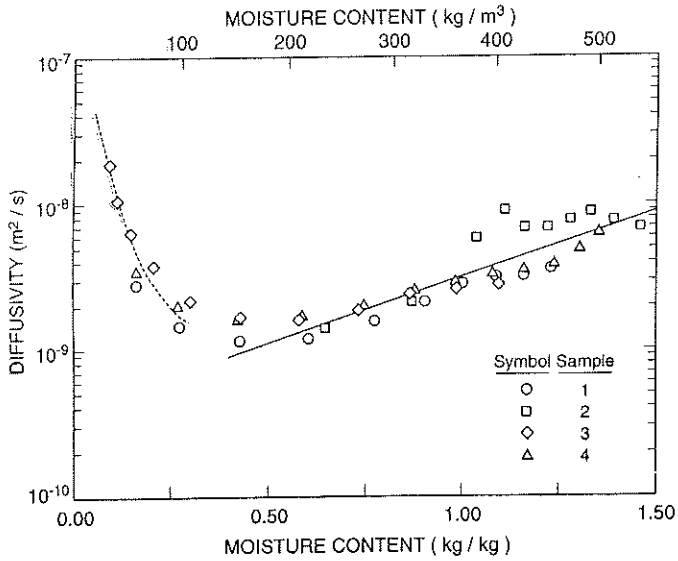

Figure 10 *Moisture diffusivity vs. moisture content for sugar pine.*

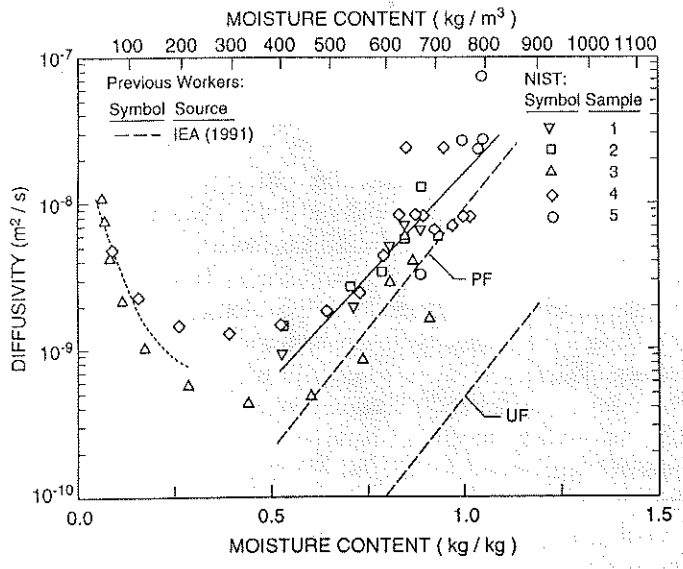

Figure 11 *Moisture diffusivity vs. moisture content for particle board with particle board correlations from IEA (particle board with urea formaldehyde [UF] resin and phenolic formaldehyde [PF] resins).*

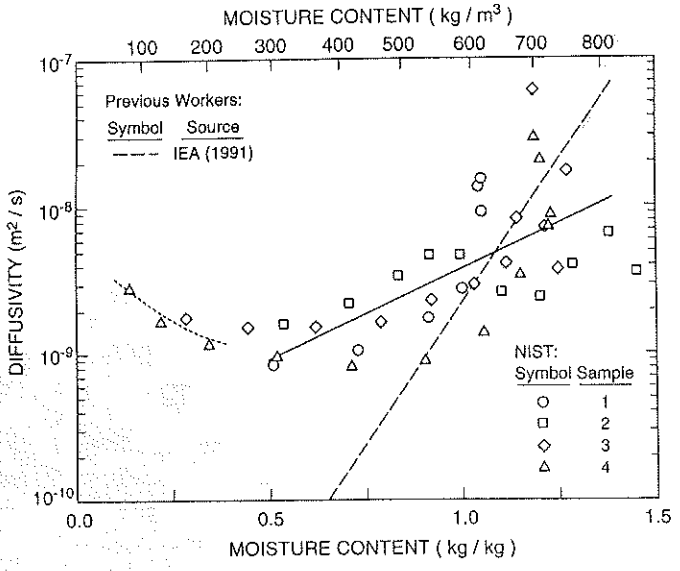

Figure 12 *Moisture diffusivity vs. moisture content for T111 sheathing with plywood correlation from IEA.*

four-point fit being swept through the moisture profile data like a sliding mean. Each profile in Figures 6, 7, and 8 thus provided a range of diffusivity data in Figures 10, 11, and 12. A discussion of the error contributors in the determination of moisture diffusivity according to this method is given in the appendix.

The moisture diffusivity data for gypsum (Figure 9) are all seen to lie along a straight line on the semi-log plot. A least-squares linear fit to the log of diffusivity gives the exponential relation

$$D(\gamma) = 7.88 \times 10^{-9} \exp(3.883\gamma), \qquad (9)$$

indicated by a solid line in the figure.

Moisture diffusivity data for sugar pine, particle board, and T111 sheathing, on the other hand, appear to fall into two distinct regimes. Looking first at the sugar pine data in Figure 10, the diffusivity data are seen to fall with increasing moisture content up until about $\gamma = 0.3$ kg/kg. For moisture contents above $\gamma = 0.4$ kg/kg, the data are seen to increase linearly with moisture content on the semi-log plot. Mass transfer in the regime of falling diffusivity at low moisture contents is often identified in the literature as dominated by vapor diffusion. At higher moisture contents, where diffusivity rises exponentially, mass transfer is believed to be dominated by surface tension driven liquid flow (Evgin and Svec 1988). A least-squares linear fit to the log of the sugar pine data at moisture contents above $\gamma = 0.4$ kg/kg gives the exponential relation

$$D(\gamma) = 3.78 \times 10^{-10} \exp(2.10\gamma) \qquad (10)$$

and is shown by a solid line in the figure. Scatter in the diffusivity data about the exponential relation is not large. The greatest variation in seen in sample 2, which rises above the rest of the data for $\gamma > 1.0$ kg/kg.

Similar behavior is seen in the data for particle board. The diffusivity data for particle board in Figure 11 drops steeply for moisture contents below $\gamma = 0.3$ kg/kg and then rises again for moisture contents above $\gamma = 0.5$ kg/kg. However, the scatter in the diffusivity data is larger than for the gypsum or sugar pine. Much of the variability seems to be due to sample-to-sample variation. For example, diffusivities found for sample 3 are consistently lower than data for the other samples at similar moisture contents. However, the variability in data from a single specimen, such as sample 4 or sample 5, is as much as a factor of four or five at higher moisture contents. The variation within samples is a consequence of evaluating the derivative of the noisy moisture profiles in Figure 7.

A least-squares linear fit to the log of diffusivity for moisture contents above $\gamma = 0.5$ kg/kg gives the exponential relation

$$D(\gamma) = 2.27 \times 10^{-11} \exp(6.53\gamma) \qquad (11)$$

and is shown with a solid line on the figure.

Diffusivities for T111 sheathing are given in Figure 12. The drop in diffusivity at lower moisture contents is much less than seen in the previous two figures. In contrast, at moisture contents above $\gamma = 0.5$ kg/kg the diffusivity is seen to rise at a rate faster than exponential for three of the four samples tested. Samples 1, 3, and 4 exhibit diffusivities that rise sharply to a cusp and then fall off. The data for sample 1 peak at a moisture content of $\gamma = 1.0$ kg/kg, while both samples 3 and 4 peak later at a moisture content around $\gamma = 1.2$ kg/kg. This kind of behavior, where the diffusivity is characterized by a broad minimum followed by a quick rise to a sharp maximum and then a sudden drop-off, has been previously reported for soils (Bruce and Klute 1956) and for concrete (Frietas et al. 1991).

For the sake of comparison, a least-squares linear fit was made to the log of the T111 diffusivity data for moisture contents above $\gamma = 0.5$ kg/kg. The fit, indicated by a solid line on Figure 12, is given by the exponential relation

$$D(\gamma) = 2.28 \times 10^{-10} \exp(2.83\gamma). \qquad (12)$$

The scatter of the data about the correlation is considerable. Large variations from sample to sample, compounded with the "cusped" behavior of the data, cause the simple exponential relation to fall short in accurately characterizing the diffusivity data.

Capillary Pressure

Capillary pressure curves for wetting only are presented in Figures 13, 14, 15, and 16. In each figure capillary suction pressure in atmospheres is plotted against moisture content. The data for two samples are plotted for gypsum, particle board, and T111 sheathing. Data from one sample of sugar pine is given.

The capillary pressure curve of gypsum (Figure 13) is seen to have a pronounced "S" shape. At a moisture content of about $\gamma = 0.5$ kg/kg, the capillary pressure falls quickly. This behavior characterizes the point of irreducible saturation. For moisture contents in the range $0.5 \text{ kg/kg} < \gamma < 1.0$ kg/kg, the curve reaches a plateau of between 0.01 and 0.02 atm. The greatest difference between the data from the two gypsum samples tested is seen in this region. Maximum saturation occurs at a moisture content of $\gamma = 1.0$ kg/kg.

The "S" shape characteristic of the gypsum capillary pressure curve is much less apparent in the data for sugar pine (Figure 14), particle board (Figure 15), and T111 sheathing (Figure 16). The three wood-based materials do not show the variation in the slopes of their capillary pressure curves that gypsum does. For these materials, capillary pressure falls more uniformly as moisture content increases. However, the scatter in the data for particle board and T111 sheathing is greater than the scatter seen in the gypsum data. Maximum sorption occurs at about $\gamma = 1.75$ kg/kg for sugar pine, at about $\gamma = 1.0$ kg/kg for the particle board, and at about $\gamma = 1.3$ kg/kg for the T111 sheathing.

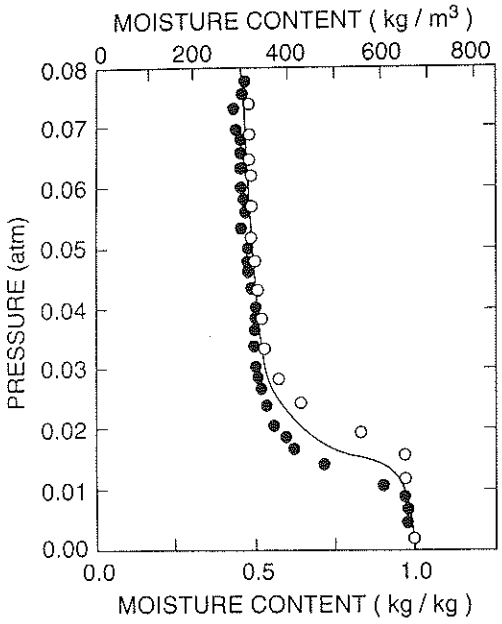

Figure 13 Capillary pressure vs. moisture content for gypsum wall board.

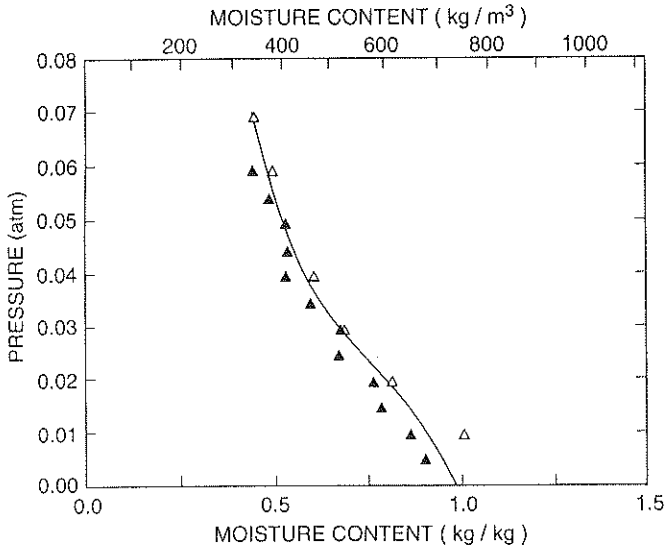

Figure 15 Capillary pressure vs. moisture content for particle board.

Comparison with Previous Work

Diffusivity data from two published sources are used for comparison with data from the present study. Moisture diffusivities measured by Gummerson et al. (1979) and correlations for moisture diffusivity tabulated by the International Energy Agency (IEA) Annex XIV (1991) are plotted in Figures 9, 11, and 12.

It is necessary to emphasize that the materials used in this study do not correspond exactly to the materials cited for comparison from the publications of Gummerson et al. and IEA. Both Gummerson et al. and IEA report dif-

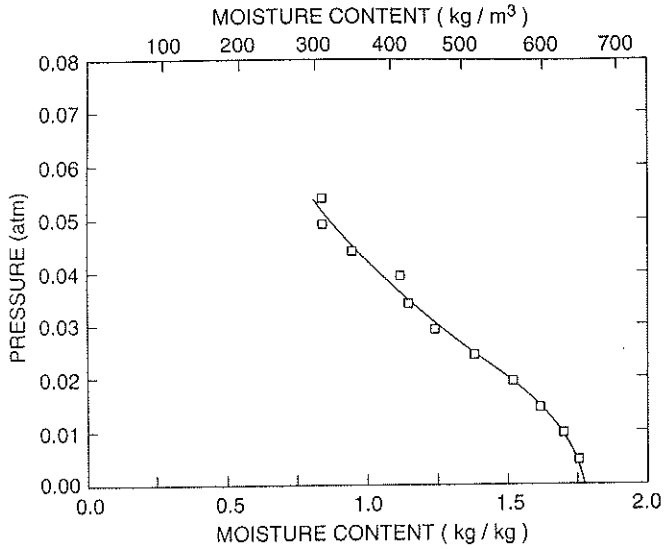

Figure 14 Capillary pressure vs. moisture content for sugar pine.

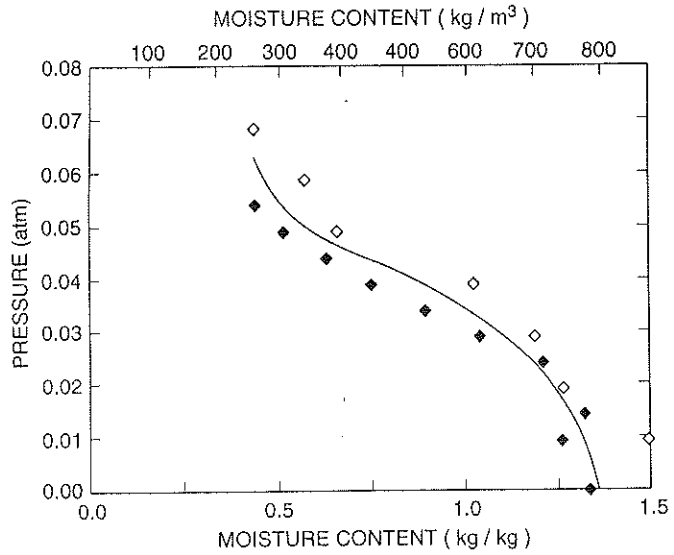

Figure 16 Capillary pressure vs. moisture content for T111 sheathing.

fusivities for gypsum plaster as opposed to the gypsum wallboard tested in this study. Likewise, the T111 sheathing and the microfine particle board from this study are not duplicates of the plywood and particle board products whose moisture diffusivities are tabulated by IEA. Nevertheless, the comparison between these similar but not identical materials is considered useful to establish ranges of moisture diffusivities for generic classes of building materials and to establish variability within those classes.

Data from Gummerson et al. and a correlation from IEA for gypsum plaster are indicated by dotted and dashed lines respectively on Figure 9. Both the data from Gummerson et al. and the IEA correlation intersect the data from the present study at moisture contents between $\gamma = 0.1$

kg/kg and $\gamma = 0.2$ kg/kg. The IEA correlation rises much faster than the present data, reaching a value of $D = 10^{-6}$ m^2/s at a moisture content of nearly $\gamma = 0.5$ kg/kg. This value of diffusivity is more than an order of magnitude larger than the data from the present study at the same moisture content. The data from Gummerson et al. increases at a rate intermediate to the IEA correlation and the data from this study. At a moisture content of $\gamma = 0.75$ kg/kg, where the present data reach a value of about $D = 10^{-6}$ m^2/s, the data from Gummerson et al. show a diffusivity of slightly less than $D = 10^{-7}$ m^2/s.

Figure 10 shows two diffusivity correlations from IEA for particle board manufactured with one of two different kinds of resin. Correlations for particle board manufactured with phenolic formaldehyde resin (PF) and for particle board manufactured with urea formaldehyde resin (UF) are shown by a dashed lines. Although both correlations are exponential, with similar slopes on the semi-log plot, there is more than an order of magnitude of difference between the two. The correlation for particle board with phenolic formaldehyde resin (PF), the larger of the two IEA correlations, is seen to pass through the lower range of the diffusivity data and somewhat below the least-squares fit from the present study. At a moisture content of $\gamma = 0.5$ kg/kg, the phenolic formaldehyde resin correlation is a factor of three lower than the least-squares fit from this study, and at $\gamma = 1.0$ kg/kg, it is about 30% lower than the least-squares fit. The correlation for particle board with urea formaldehyde resin lies well below the data from the present study.

The IEA correlation for the moisture diffusivity of plywood is indicated in Figure 12 with a dashed line. It is shown alongside data and the least-squares fit to the data for the T111 sheathing from the present study. The IEA exponential correlation has a much larger slope on the semi-log plot than the least-squares fit to the T111 data from the present study. At low moisture contents, below $\gamma = 0.5$ kg/kg, the moisture diffusivity predicted by the IEA correlation is more than an order of magnitude lower than the present data show. At high moisture contents above $\gamma = 1.25$ kg/kg, the IEA correlation rises significantly above the present data. The IEA correlation falls within the scatter of the data from this study over a wide range of moisture contents (0.8 kg/kg $< \gamma < 1.2$ kg/kg) because of the large variability in diffusivity found in the four T111 sheathing samples.

Sorptivity

Sorptivities were measured directly for each of the materials in this study. As described above, Equation 8 was fitted to the initial transient data in Figures 3 and 4 using least-squares linear fits. Two values of sorptivity, one for each specimen in the figures, were determined for each of the materials. The values of sorptivity, S, determined from these line fits are listed in Table 1 under the heading "Measured S."

TABLE 1
Measured and Predicted Sorptivities ($m/\sqrt{s}$)

Material	Measured S (Low)	Measured S (High)	Predicted S
Gypsum	1.5×10^{-4}	1.7×10^{-4}	2.7×10^{-4}
Sugar Pine	6.6×10^{-5}	8.9×10^{-5}	9.6×10^{-5}
T111 Sheathing	5.4×10^{-5}	6.4×10^{-5}	5.6×10^{-5}
Particle Board	2.9×10^{-5}	2.1×10^{-4}	4.4×10^{-5}

In addition, sorptivity was predicted using the exponential correlations for moisture diffusivity (Equations 9, 10, 11, and 12) developed for the four sample materials. Employing Equation 6, the Brutsaert approximation, in conjunction with the exponential correlations gives the predicted sorptivities, S, for the four tested materials. These values of sorptivity are given in Table 1 under the heading "Predicted S."

The measured sorptivity data give an impression of the sample variability possible in building materials of the type tested. In three out of four materials (gypsum, sugar pine, and T111 sheathing), the sorptivities measured for two test specimens of each material are within 35% of one another. In contrast, the two measured particle board sorptivities differ by almost a factor of ten. However, the very small number of specimens tested makes it difficult to generalize from these limited results.

Consideration of the particle board sorptivity data is instructive. Referring back to Figure 4 will remind the reader that the lower value of sorptivity was measured for sample 3 of the particle board while the higher sorptivity was measured for sample 5. In Figure 11, the measured moisture diffusivity data for sample 3 is seen to be substantially lower over the entire range of moisture contents than the moisture diffusivity measured for sample 5. A lower diffusivity should imply a lower sorptivity, since sorptivity is a measure of diffusivity integrated over a range of moisture contents. This connection between sorptivity and diffusivity has been described by Hall et al. (1983) and Wang and Fang (1988). The data for particle board specimens 3 and 5 suggest the value of sorptivity as a simple test of sample variability in moisture diffusivity.

Table 1 also shows predicted sorptivities. The predicted sorptivities are higher than measured sorptivities for the gypsum and sugar pine specimens and fall between the high and low sorptivities measured for the particle board and the T111 sheathing specimens. The predicted sorptivity is 60% to 80% higher than the measured sorptivities for gypsum and between 10% and 45% higher than measured values for sugar pine. Given the level of uncertainty in the diffusivity measurements and the scatter in the diffusivity data, discrepancies of this magnitude are not unexpected.

CONCLUSIONS

Moisture transport properties have been measured for four common building materials: gypsum wall board, sugar

pine, microfine particle board, and T111 sheathing. The time history upon exposure to free liquid, the sorptivity, the one-dimensional moisture content profiles under steady-flux conditions, moisture diffusivity as a function of moisture content, and capillary pressure curves for low suction pressures have been presented for each material. Exponential correlations have been fitted to the moisture diffusivity data for gypsum and sugar pine with good success and to the diffusivity data for particle board and T111 sheathing with much less success.

The scatter in both the measured moisture profiles and moisture diffusivities is large. The uncertainty inherent in the experimental technique, especially due to the necessity of finding the derivative of noisy experimental data, contributes to the wide range of diffusivities measured. In addition, sample-to-sample variability appears to be significant. Unfortunately, the very limited number of specimens tested makes generalizations about sample variation impossible. The diffusivities found in this study compared with results published by Gummerson et al. (1979) and IEA (1991) for similar but not identical materials within an order of magnitude.

Sorptivities predicted using the Brutsaert approximation and the exponential correlations for each of the four materials were compared to sorptivities measured from the transient data. For the few specimens considered, the comparison was fair. In the case of particle board, sorptivity appeared to be a useful indicator of sample variability in moisture diffusivity.

ACKNOWLEDGMENTS

The author would like to thank the Office of Buildings and Community Systems of the Department of Energy for funding this research. In addition the author gratefully acknowledges John Judge and Kevin Simmons for their ready assistance in cutting and weighing the specimens and Doug Burch for his very helpful comments, criticisms, and advice.

NOMENCLATURE

a = cross-sectional area, m^2
b = constant in Equation 8, kg
c = constant in Equations 5 and 6, dimensionless
D = moisture diffusivity, m^2/s
m = mass flux, $kg/(m^2 \cdot s)$
M = mass, kg
S = sorptivity, $m/\sqrt{s}$
t = time, s
x = distance from sample tip, m
γ = moisture content, kg/kg
η = Boltzmann similarity variable, $m/\sqrt{s}$
ρ = density of water, 1000 kg/m^3

Subscripts

d = dry
w = wet
s = solid matrix
sat = saturated

REFERENCES

Ambrose, J.H., L.C. Chow, and J.E. Beam. 1990. "Capillary flow properties of mesh wicks." *AIAA J. Thermophysics* 4: 318-324.

Arfvidsson, J., and J. Claesson. 1989. "A PC-based method to calculate moisture transport." International Symposium ICHMT, Dubrovnik, Yugoslavia.

Bruce R.R., and A. Klute. 1956. "The measurement of soil moisture diffusivity." *Soil Sci. Soc. Am. Proc.* 20: 458-462.

Brutsaert, W. 1976. "The concise formulation of diffusive sorption of water in a dry soil." *Water Resources Research* 12: 1118-1124.

Burch, D.M., and W.C. Thomas. 1991. "An analysis of moisture accumulation in a wood frame wall subjected to winter climate." NISTIR 4674, National Institute of Standards and Technology, Washington D.C.

Burch, D.M., W.C. Thomas, and A.H. Fanney. 1992. "Water-vapor permeability measurements of common building materials." *ASHRAE Transactions* 98.

Choong, E.T., and F.O. Tesoro. 1989. "Relationship of capillary pressure and water saturation in wood." *Wood Science and Technology* 23.

Evgin, E., and O.J. Svec. 1988. "Heat and moisture transfer characteristics of compacted MacKenzie silt." *Geotechnical Testing Journal*, 92-99.

Freitas, V., P. Crausse, and V. Abrantes. 1991. "Moisture diffusion in thermal insulating materials." *Insulation Materials: Testing and Applications, 2, ASTM STP 1116*, R.S. Graves, and D.C. Wysocki, eds. Philadelphia: American Society for Testing and Materials.

Gummerson, R.J., C. Hall, W.D. Hoff, R. Hawkes, G.N. Holland, and W.S. Moore. 1979. "Unsaturated water flow within porous materials observed by NMR imaging." *Nature* 281:56-57.

Gummerson, R.J., C. Hall, and W.D. Hoff. 1980. "Water movements in porous building materials—II. Hydraulic suction and sorptivity of brick and other masonry materials." *Building and Environment*, 15:101-108.

Hall, C., W.D. Hoff, and M. Skeldon. 1983. "The sorptivity of brick: Dependence on the initial water content." *J. Physics D: Applied Physics* 16:1875-1880.

IEA (International Energy Agency). 1991. "Catalogue of Material Properties." Report Annex XIV, Condensation and Energy, 3.

Kohonen, R. 1984a. "Transient analysis of the thermal and moisture physical behaviour of building constructions." *Building and Environment* 19:1-11.

Kohonen, R. 1984b. "A method to analyze the transient hygrothermal behaviour of building materials and components." Technical Research Centre of Finland, pub. 21, Espo.

Kumaran, M.K., and M. Bomberg. 1985. "A gamma-spectrometer for determination of density distribution and moisture distribution in building materials." *Proc. Intl. Symp. on Moisture and Humidity, Wash. D.C.*, 485-490.

Pedersen, C.R. 1990. "Combined heat and moisture transfer in building constructions." Report no. 214, Thermal Insulation Laboratory, Technical University of Denmark.

Prazak, J., J. Tywoniak, F. Peterka, and T. Slonc. 1990. "Description of transport of liquid in porous media—A study based on neutron radiography data." *Int. J. Heat Mass Transfer* 33:1105-1120.

Quenard, D., and H. Sallee. 1989. "A gamma-ray spectrometer for measurement of the water diffusivity of cementitious materials." *Mat. Res. Soc. Symp. Proc.*, 137.

Richards, R.F., D.M. Burch, and W.C Thomas. 1992. "Water vapor sorption measurements of common building materials." *ASHRAE Transactions* 98.

Spolek, G.A., G.R. Osterhout, and R.I. Apfel. 1985. "Transient heat and mass transfer in walls." *Thermal Performance of the Exterior Envelopes of Buildings III*, ASHRAE/DOE/BTECC, Clearwater Beach, Florida.

Spolek, G.A., and O.A. Plumb. 1981. "Capillary Pressure in Softwoods." *Wood Science and Technology*, 15.

Wang, B. and Z. Fang. 1988. "Water absorption and measurement of the mass diffusivity in porous media." *Int. J. Heat Mass Transfer* 31:251-257.

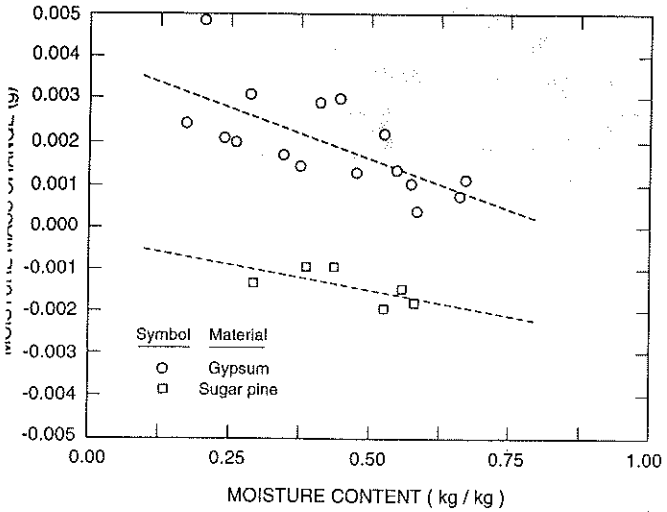

Figure 17 Moisture mass change vs. sample moisture content due to "cut and weigh" technique for sugar pine and gypsum samples.

APPENDIX

Uncertainty

Uncertainty was introduced into the moisture diffusivity data from three sources: errors in moisture content measurements, errors in slice postion, and errors in the measurement of mass flux through the specimens.

Error in the measurement of moisture content due to the cutting and weighing operation was determined in a separate experiment. Samples of gypsum and sugar pine were initially dried over desiccant and weighed to find their dry mass. Water was then added to the specimens to bring them to predetermined moisture contents. The specimens were allowed to sit undisturbed for a sufficient length of time to ensure the moisture content in each was uniform. For the case of gypsum, 24 hours were deemed sufficient, and for the case of sugar pine, several days were allowed. The samples were weighed again to establish their wet masses and then immediately frozen in liquid nitrogen. The procedure of cutting into slices, weighing, desiccating, and weighing again was exactly as has been previously described for the steady-flux specimens used in the moisture content profile measurements. By measuring wet and dry mass before cutting and after cutting, it was possible to determine the mass of dry specimen and the mass of water lost or gained during cutting. Figure 17 shows the results of the experiment. In the figure, the change in the mass of water measured in samples before and after cutting is plotted versus moisture content for both gypsum and sugar pine samples.

The change in moisture mass inadvertently caused by slicing the samples is seen to introduce both systematic and random errors into the moisture content measurements. Overall, the gypsum samples gained a little water, probably from condensation on the frozen specimens. The trend of the data is downward, however, suggesting competing mechanisms of water gain and loss, with water loss growing as moisture content increases. The sugar pine samples all lost water mass with the same downward trend in the data.

We are chiefly interested in random errors because systematic errors in moisture content do not contribute to uncertainty in the derivative in Equation 6. For both the gypsum and the sugar pine samples, the random component of uncertainty due to cutting is less than ± 0.002 g. The nominal mass of a gypsum slice was 0.5 g and the nominal mass of a sugar pine slice 0.3 g. The random uncertainties in moisture content for gypsum and sugar pine can therefore be estimated at 0.004 kg/kg and 0.007 kg/kg, respectively.

A second source of uncertainty in the diffusivity data was due to errors in the determination of the positions of the measured local moisture contents. The location of the measured moisture contents was determined by adding up slice thickness. Slice thickness, measured by micrometer, had an estimated fractional uncertainty of ± 0.05 for gypsum and ± 0.04 for the sugar pine.

The final contributor of uncertainty was due to error in the measurement of mass flux through the material samples. Figures 3 and 4 illustrate the minimal scatter typical of the mass flux measurements made for both the sugar pine and gypsum samples. Line fits to the mass versus elapsed time data yielded slopes (mass fluxes) with fractional uncertainties (95% confidence intervals) of only ± 0.04 for the gypsum samples and ± 0.02 for the sugar pine.